Numerical Simulation and Seismic Performance of Buckling Instability of Piles in Liquefiable Ground

Muhammad Hamzah Fansuri[1], Muhsiung Chang[2], Rini Kusumawardani[3], Togani Cahyadi Upomo[4]

[1]Master Student, Dept. Civil & Construction Engineering, National Yunlin Univ. of Sci. & Tech. (YunTech), Yunlin, Taiwan
[2]Professor, Dept. Civil & Construction Engineering, National Yunlin Univ. of Sci. & Tech. (YunTech), Yunlin, Taiwan
[3]Assoc. Professor, Dept. Civil Engineering, Universitas Negeri Semarang (Unnes), Semarang, Indonesia
[4]PhD Student, Dept. Civil & Construction Engineering, National Yunlin Univ. of Sci. & Tech. (YunTech), Yunlin, Taiwan

Abstract

The paper discusses an alternative to compute and analyze pile buckling in liquefiable ground during seismic shaking. This study is undertaken based on three-dimensional finite element (FE) simulations using OpenSeesPL. To explore the effect of shaking, soil and pile behaviors are observed at different axial loading conditions. The results reveal insights of axial load influence due to soil liquefaction in both near-field and free-field grounds. Analysis results show that an increase in axial load would generally decrease the lateral displacement and increase the bending moment of piles, as well as reduce the acceleration and excess pore pressure responses in soils by seismic shaking and soil liquefaction. From the case examined in this study, we notice the computed bending moments in piles are less than that of the yielding or ultimate moment, which appear dissimilar results by using Bhattacharya's approach that would indicate the buckling of piles under the dynamic axial loads and soil liquefaction in seismic shaking. Further studies would therefore be warranted to justify the capability and suitability of the numerical simulations conducted herein. Nonetheless, the revealed insights by numerical simulations provide a good basis for understanding and analysis on the buckling of piles in liquefiable ground.

Keywords: Pile buckling; Seismic shaking; Soil liquefaction; Numerical simulation; OpenSeesPL

Introduction

Soil liquefaction is one of complex phenomena that causes many damages during earthquakes. In addition, liquefaction represents one of the biggest contributors to the damage of constructed facilities during earthquakes; for instances, settling, tilting, and sliding of building structures due to soil liquefaction.

Liquefaction of soils has caused considerable damages to pile-supported structures such as bridges and buildings. Liquefaction was reported as the main cause of damages to pile foundations during major earthquakes, such as 1964 Alaska, 1989 Loma-Prieta, 1995 Hyogoken-Nambu (Kobe), 1999 Chi-Chi, 2011 Tohoku earthquakes (Kramer 1996; Finn & Fujita 2002, EERI 1999, Bhattacharya et al. 2013). Recently, Palu earthquake, Indonesia, on 28 September 2018 with a magnitude (M_w) of 7.5 caused strong shaking, generating a tsunami and massive liquefaction (GEER 2019).

The strength and stiffness of soils decrease due to the increase in pore pressure by earthquake shaking and would seriously affect the embedded piles, causing large bending moments and shear forces and eventually threatening structural stability of the piles.

Generally, soil profiles encountered for piles consist of a liquefied layer sandwiched between a non-liquefied crust and a non-liquefied base layer (Cubrinovski & Ishihara 2005).

The collapse of pile structures is observed after many strong earthquakes due to lack of safety factor against bending failure by the lateral or axial loading. Several methods are available for calculating the bearing capacity of pile foundations, such as theoretical formulas based on static analysis (Kulhawy 1984; Poulos 1989), in-situ testing (Meyerhof 1976; Schmenrtmann 1978; Eslami and Fellenius 1997), dynamic approach (Goble and Rausche 1979; Rausche et al. 1985; Fellenius 2006), or through interpretation of full-scale pile load tests (Fellenius 1990).

Piles must be designed to sustain axial (vertical) and lateral (horizontal) loads without suffering structural damages, bearing capacity failures and excessive settlements or deflections.

Terzaghi (1943) has proposed a theory for calculating the bearing capacity of shallow foundations by the following:

$$q_{ult} = cN_c + qN_q + 0.5\gamma BN_\gamma \quad (1)$$

where q_{ult} is the ultimate bearing capacity, c is cohesion, q is surcharge pressure, B is the foundation width, γ is the soil unit weight, and N_c, N_q, and N_γ are bearing capacity factors that are the functions of soil friction angle. For deep (pile) foundations the third term can usually be neglected because of relatively small width (diameter) of the pile (Bowles, 1996). Thus, the ultimate base capacity of pile is regarded as $cN_c + qN_q$. Except for pre-consolidated clays and cemented sands, the above equation can take the form qN_q.

A pile under axial load derives its load-carrying capacity through the friction or adhesion along the pile shaft and by the compressive resistance at the pile base with underlying soils (Salgado, 2008). The ultimate bearing capacity Q_{ult} of single pile may be expressed as:

$$Q_{ult} = \ Q_b + Q_s = q_b A_b + \sum_{i=1}^{n} q_s A_s \qquad (2)$$

where Q_b is base resistance, Q_s is limit shaft resistance, q_b is unit base resistance, q_s is limit unit shaft resistance, A_b is area of pile base, and A_s is pile shaft area.

Bhattacharya and Madabhushi (2008) suggested that the bending moment or shear force experienced by the failed piles due to soil liquefaction of lateral spreading would exceed the bending or shear carrying capacity of the piles.

Pile foundations in liquefiable soils subjected to seismic shaking may also due to excessive settlements. The mechanism of buckling instability in liquefiable soils has been proposed (Bhattacharya 2003; Bhattacharya et al. 2004; Knappett and Madabhushi 2005; Kimura and Tokimatsu 2005; Shanker et al. 2007). During liquefaction, the pile would suffer a significant loss lateral support in the liquefied zone, Therefore, if the axial load is close to its critical buckling load, then buckling instability of piles may occur, which would be promoted by the actions of lateral load or material imperfection.

Bhattacharya (2015) described that prior to shaking the axial load acts on pile beneath a building is equally distributed under static conditions without any eccentricity of loading. During earthquake shaking, the inertial action of superstructure imposes dynamic axial loads on the piles, which can be given by the following:

$$P_{dynamic} = P_{static} + \Delta P = (1 + \alpha)P_{static} \quad (3)$$

where α is the dynamic axial load factor, which is a function of the type, dimension and mass of the superstructure, the characteristics of seismic shaking, as well as material properties and geometry of the pile foundation.

In the following, a brief description will be given on the geotechnical problems and code requirements for pile design under static and seismic loadings. In such cases, modification methods would be called upon to reach the level of improvement that is needed. Attaining necessary improvements against buckling instability in liquefiable ground may sometimes be difficult and expensive.

In this regards, numerical simulations can provide an important role for the development of an economical and effective solution. This paper proposes numerical simulations to evaluate soil-pile responses due to seismic shaking, and behaviors of pile buckling during soil liquefaction.

Literature review

JRA (1996) describes that certain soils liquefy during earthquake shaking, losing their shear resistances and causing flow with overlying non-liquefied crust. The mechanism and criteria to be used by practicing engineers are usually specified by prevailing codes. An example is the bending failure of piles by assuming non-liquefiable crust offers passive resistance and liquefied soil layer offers restraint equal to 30% of the overburden pressure.

Bhattacharya et al. (2004) proposed an alternative mechanism of pile failure in liquefiable deposits during earthquake. It has been demonstrated that the end-bearing piled foundations can be vulnerable to buckling instability during seismic liquefaction based on the results of centrifuge tests. Their works considered that the pile becomes unstable under axial load from loss of support from the surrounding liquefied soil, provided the slenderness ratio of the pile in unsupported zone exceeds a critical value. The instability causes the pile to buckle and causes a plastic hinge in the pile. In a soil-pile interaction term, the method assumes that, during instability, the pile pushes the soil. Consequently, the lateral load effect is considered secondary to the basic requirements that piles in liquefiable soils must be checked against Euler's buckling.

If the pile buckles due to diminishing effective stress and shear strength of soils owing to liquefaction, buckling instability can be a possible failure mechanism irrespective of level or sloping ground.

Foundations directly supported on soil are particularly vulnerable to liquefaction. This phenomenon is well understood and studied. Piled foundation responses to liquefaction and buckling are less studied.

Designing piles with column buckling and beam bending criteria require different approaches. Dash et al. (2010) described the former is based on strength and the latter is on stiffness. Bending failure depends on the bending strength, such as moment at first yield (M_y), and plastic moment capacity (M_p) of the pile. While buckling represent a sudden instability of the pile when axial load reaches the critical value (P_{cr}).

Bhattacharya & Goda (2013) proposed the probabilistic evaluation of liquefaction-induced pile foundation buckling failure due to a scenario earthquake. By comparing critical pile length (H_c) and unsupported pile

length (D_L), the potential failure of the pile due to buckling is indicated when $H_c < D_L$. The unsupported length (D_L) can be assessed based on the depth interval of liquefied soils plus some fixity (normally 3~5 times the pile diameter). The critical pile length (H_c) can be computed by the Euler's theory as below:

$$H_C = \sqrt{\frac{0.35\pi^2 EI}{K^2 P_{dynamic}}} \quad (4)$$

where K is the Euler's effective column length coefficient, depending on the boundary condition of column. Finally, buckling index (G) can be defined by following:

$$G = H_C - D_L \quad (5)$$

Based on Eq. (5), if G is greater than zero (i.e., $H_C > D_L$), then pile is considered safe. Otherwise, the pile will be buckling due to seismic loading and soil liquefaction.

On the other hand, some researchers use numerical simulations to model the liquefaction-induced pile failure during shaking, with aims to mitigate detrimental liquefaction effects with various kinds of modification techniques (Mitchell et al. 1998; Adalier and Elgamal 2004). Installation of piles to mitigate lateral spreading effects has been proposed (Boulanger and Tokimatsu 2005; Boulanger et al. 2007). During and after earthquake shaking, liquefaction of mitigated ground would be affected by several key parameters (e.g. area replacement ratio, soil and stone column permeability, pile or stone column diameter, mass of the superstructure and ground motion characteristic) and may result in localized deformation (Kokhuso 1999; Yang and Elgamal 2002; Asgari et al. 2013).

Elgamal et al. (2009) conducted simulations by using OpenSeesPL to evaluate mitigation of soil liquefaction by stone column (SC) and pile-pinning approaches on the basic of a systematic parametric study. Recently, the simulation of pile buckling is considered due to axial loading during seismic excitation. It is important to know the behaviors surrounding soil and pile during the seismic excitations.

Numerical simulations

Analysis framework

The simulations are carried out by using the open-source computational platform, OpenSees (Mazzoni et al. 2006; McKenna et al. 2010). The platform allows for developing application to simulate performance of structures and geotechnical systems subjected to static and seismic loadings. The 3D finite-element modeling of the soil is represented by 20-8-node brick elements. The nodal element is based on the solid-fluid formulation with saturated soil implementation in OpenSees.

The OpenSeesPL approach is adopted in this study (http://cyclic.ucsd.edu/openseespl). It has particular capabilities for carrying out a large variety of 3D finite-element simulations based on the OpenSees computational platform (Lu 2006; Elgamal et al. 2009). In addition to static analysis, the software allows for dynamic and cyclic earthquake simulations with linear, bilinear, or advanced (i.e., nonlinear fiber) element formulations.

Wang (2015) described that OpenSeesPL allows for simulating with considerations to: (1) convenient generation of the mesh (e.g., surface load/axial/footing, single pile, pile group) and associated boundary condition; (2) simplified selection of soil/pile linear/non-linear material modeling parameters in finite-element input file (Yang et al. 2003; Elgamal et al. 2008); (3) execution of simulation using an OpenSees platform; (4) single pile and pile group computations under seismic shaking as well as studies in prescribed displacement or prescribed force modes; (5) numerical studies in various ground modification scenarios by using certain specification of material within pile zone (Elgamal et al. 2009; Asgari et al. 2013; Lu et al. 2019); (6) graphical display of the results for footing or pile and ground system.

Analysis procedure

The model adopted in numerical analyses is shown in Fig. 1. All simulations were developed and executed using interface OpenSeesPL based on $u - p$ formulation. The 3D finite-element soil domain is represented by 8-node, fully-coupled (solid-fluid) brick elements. In this scenario, an 18-m thick saturated sand layer was studied, with a permeability k = 6.6×10^{-5} m/s based on Nevada sand properties at a medium relative density D_r of approximately 40% (Elgamal et al. 2009; Asgari et al. 2013; Lu et al. 2019) and performed with a groundwater level of 0.9 m below ground surface. The ground surface was assumed level.

In the following, the plane area of simulation was 4.6 m × 4.6 m (square area), and the scenarios were analyzed using same meshes with spacing of 1 m in longitudinal (x), transverse (y) and vertical (z) directions. In terms of base excitation (embedded at 18-m depth), the downhole north-south (N-S) acceleration record from El Centro earthquake (1940) was adopted along the x-axis, as shown in Fig 2.

To explore the effect of seismic shaking on soil and pile behaviors, different axial loadings on the pile were considered, including 0, 1500, 3000, and 6000 kN. In addition, simulation results were examined for the behavior of soils in near-field and free-field.

Example case description

In this study, a series of numerical analysis was carried out to investigate various factors affecting on the liquefaction potential of saturated soil, the axial load transfer mechanism, and the seismic performance of

pile foundation. Therefore, using a comprehensive constitutive soil model is one of the most important parts of numerical simulation of dynamic behavior of liquefiable soils.

In view of symmetry, only half-mesh was performed with lateral loads applied along the longitudinal of the model. According to Tang et al. (2015), the following aspects were considered: (1) the penalty method was used to set equal degree-of-freedom (DOF) of displacements for the left and right boundaries at any spatial location in horizontal and vertical directions (i.e., periodic-boundary); (2) due to symmetry, the inner and outer boundaries were fixed against out-of-plane displacement but free to move longitudinally and vertically; (3) the ground surface was stress-free; (4) the seismic excitation was imposed at the base along the x-axis (longitudinal) direction.

One of the parameters in this modeling lies in soil type. The physical and mechanical properties of soil layer and reinforced concrete pile are presented in Tables 1 & 2, respectively. The exterior and interior diameters of reinforced concrete pile are 600 mm and 400 mm, respectively. Rigid beam-connections, normal to the pile longitudinal axis, were used to represent the geometric space occupied by the pile. The soil domain's 3D brick elements are connected to the pile geometric configuration at the outer nodes of these rigid links using the equal DOF constrain in OpenSees for translation only (Asgari et al. 2013).

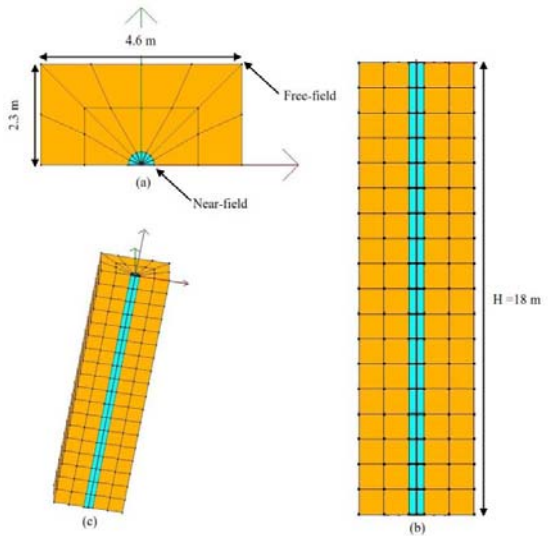

Fig.1. FE mesh for the ground modification study: (a) schematic plan view; (b) side view; (c) 3D isometric view (soil stratum with half mesh employed due to symmetry).

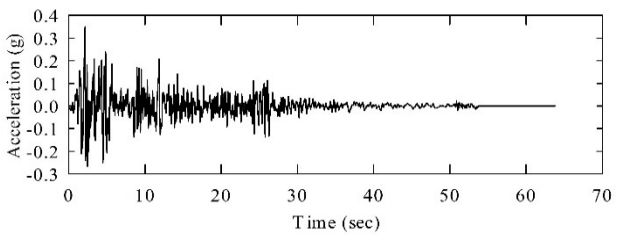

Fig. 2. Base input motion (El Centro earthquake of 1940)

Table 1. Soil parameters

Parameters	Medium
Mass density γ_m	1900 kg/m^3
Low-strain shear modulus G_r	78.5 MPa
Friction angle ϕ	31.4^o
Liquefaction yield strain γ_y	1%
Contraction parameter c_1	0.3
PT angle ϕ_{PT}	26.5^o
Dilation parameter d_1	0.4
Dilation parameter d_2	2.0

Table 2. Reinforced concrete pile parameters

Parameters	Reinforced concrete pile
Weight of concrete γ_c	2.5 Mg/m^3
Yielding moment M_y	908 kN-m
Plastic moment M_u	1317 kN-m
Flexural rigidity EI	178×10^3 kN-m^2
Shear rigidity GA	228×10^4 kN-m^2
Torsional rigidity GJ	23×10^3 kN-m^2
Axial rigidity EA	546×10^4 kN-m^2

Table 3. Earthquake data

Earthquake motion parameters	El Centro (USA)/N-S
Date of occurrence	18/05/1940
Recording station	117 EL Centro
Moment magnitude of earthquake M_w	7.1
Max. horizontal acceleration MHA	0.314 g
Predominant period T_p	0.5 sec
Bracketed duration	28.78 sec
Significant duration D_{5-95}	23.84 sec
Time of MHA t_p	2 sec
PGV/PGA	0.113 sec
Arias intensity for scaled PGA=0.35 g	2.175 m/sec
Energy flux for scaled PGA=0.35 g	2469 Jm^{-2}sec^{-1}
No. of significant excitation cycles N_c	14.5

The numerical simulations were performed with different the axial loads (i.e. vertical dead loads) at the center of pile head, with 0, 1500, 3000, and 6000 kN, to demonstrate the effect of non-linear soil response and to compare their influences on soils in the near and free fields.

To examine the characteristics of input motions, we adopted a strong shaking phase of the downhole N-S acceleration record and embedded at an 18-m depth of the model. The shaking data was based on El Centro earthquake (1940), which had caused large ground failures and extensive liquefaction phenomena. The earthquake data for this study are shown in Table 3.

Simulation results

1. Soil response of shaking

Acceleration amplitude appears to increase as the depth of soil becomes shallower, as shown in Fig. 3. It is also noticed that the increase in axial load of pile would generally decrease the acceleration responses in soil. The acceleration responses does not differ much, however, for the soils in near-field (i.e., at the contact

with pile) and free-field (i.e., at the edge of model). A more "rigor oscillation" would appear noted for soils in the near-field of this study.

The study here demonstrates the soil deposit would tend to amplify the seismic shaking. As the increase in the axial loading on pile, a situation similar to a heavier superstructure, the natural period of the pile structure would be increase, and hence less interaction between pile and soil. In accordance, the increase in axial loading on pile would reduce the acceleration response in soil. It can be perceived that the soil along the contact of pile (i.e., near-field) would be subjected to more interaction effect than that of the soil in a distance away (i.e., free-field). And hence the response of soil in free-field would tend to be smoothened.

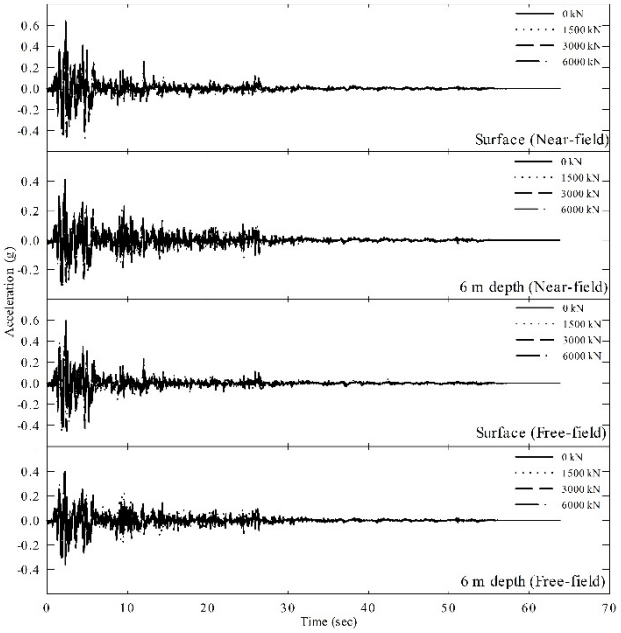

Fig. 3. Acceleration time histories at surface and 6-m deep for soils in near and free fields.

2. Behavior of soil

Fig. 4 shows excess pore pressure responses in soils. Generally, the excess pore pressures reach their original effective stresses (i.e., soil liquefaction) at shaking times of approximately 5 and 10 seconds, respectively, for soils at depths of 6 and 12 meters, indicating soil liquefaction would be generated at a shallower depth and then propagated downwards. Through a series of excess pore pressure response with depth, we would be able to determine the depth interval of liquefied soil or the unsupported length of pile (D_L).

It is noticed that the near-field responses in excess pore pressure are apparently more "rigorous" than that in the free-field. Due to the interaction effect as mentioned previously, the excess pore pressure responses would be smoothened for the soils in a distance away from the pile.

In the figure, we also observe a delayed response in excess pore pressure as the increase in axial load on pile. The increase in axial load of pile would postpone the development of excess pore pressure, and thus the occurrence of soil liquefaction. For instance, liquefaction of soil in free-field and at a depth of 12m occurs at shaking times of approximately 10, 12 and 18 seconds, respectively, for axial loads of pile of 0, 1500 and 3000 kN. For the axial load of 6000 kN, however, the free-field soil at 12m deep would never liquefy during the course of input seismic shaking.

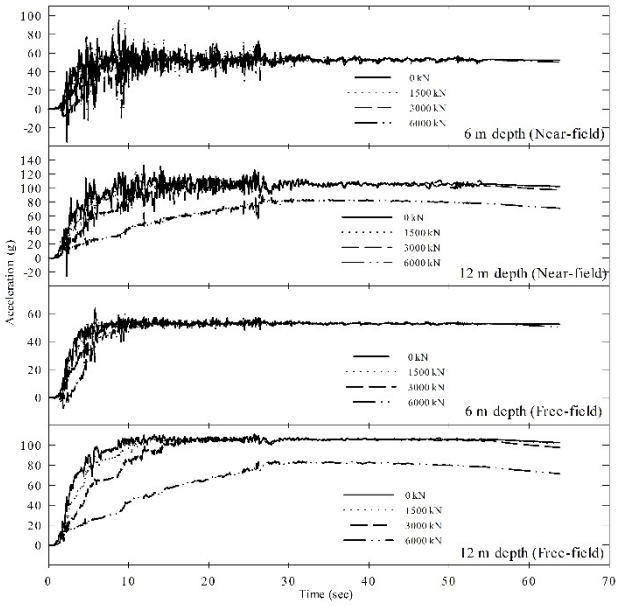

Fig. 4. Excess pore pressure time histories at surface and 6-m deep for soils in near and free fields (initial effective stresses at 6 and 12 m depths are 64 and 119 kPa, respectively).

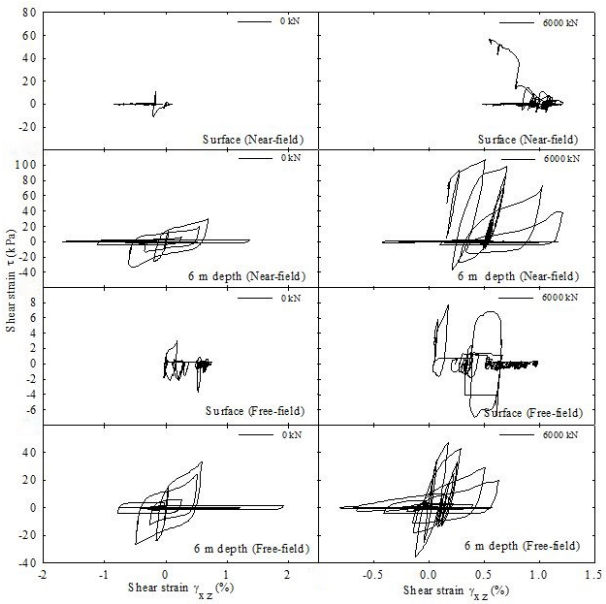

Fig. 5. Shear stress-strain relationships at surface and 6-m deep for soils in near and free fields.

Fig. 5 shows the shear stress vs. shear strain relationships of soils in the near and free fields and with different axial loads of pile. The stress-strain hysteresis loops will become flattened as the soil is weakened or softened as due to the developed excess pore pressure in

soil. Eventually, the sandy soils would be liquefied and the corresponding stress-strain curves will show large strains with negligible shear resistances.

As shown in the figure, the increase in pile axial load would generally reduce the aforementioned interaction effect, a less response in excess pore pressure, and thus a stiffer stress-strain relationship in soil. It is also noticed that the deeper the soil the stiffer would be the stress-strain relationship for soil, a situation can also be explained by the delayed development of excess pressure with depth during seismic shaking.

Due to its close proximity to the pile, the near-field soil would suffer more interactive effect, higher response in excess pore pressure, and thus less stiff in the stress-strain relationship of soil, as shown in the figure.

3. Behavior of the pile

Lateral displacement of pile during seismic shaking is examined for the cases with various axial loads and at different depths of concern. As indicated in Fig. 6, the lateral displacement of pile would be decreasing with the depth of concern, suggesting the lateral displacement of pile due to shaking would be amplified or maximized at the pile head.

As far as the effect of axial load, we notice that the increase in the pile axial load would tend to reduce the lateral displacement of the pile. Since the increase in axial load of pile would be similar to the increase in the weight of superstructure, the lateral displacement of pile would therefore be reduced as due to the increasing axial pile load. The effect of axial pile load will be further discussed in the following paragraphs.

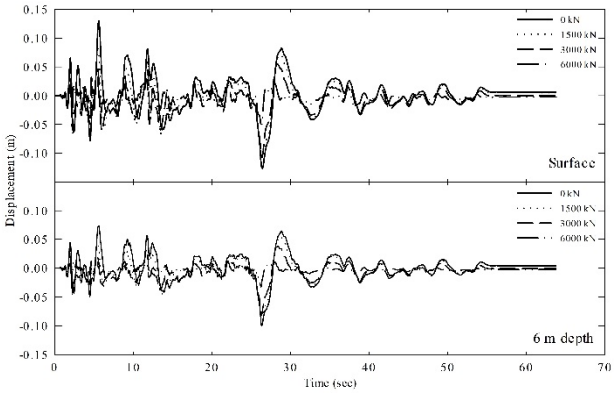

Fig. 6. Displacement vs. time histories of pile at the surface and a depth of 6-m.

The weights from superstructure are transferred to the pile, which is eventually considered as the axial or pile head loads. The pile head load will affect the responses of pile during seismic shaking in terms of lateral displacement, shear force and bending moment profiles. Figs. 7 and 8 show the results of pile response profiles due to various axial pile loads at the end of shaking and the maximum profiles during the shaking, respectively.

As shown, the increase in axial loading would generally decrease the lateral displacement of pile, both at the final stage of shaking and the maximum profile throughout the shaking history.

Results indicate the increase in pile axial loading would normally increase the shearing force in pile due to the shaking. The maximum shear would appear to locate at the fixed-end pile tip.

For the bending moment in pile, we observe that the maximum moments would also occur at the fixed-end pile tip, same as for the maximum shears. Except for the zero-axial-load case, the maximum moment vs. depth profiles would be similar for the piles with axial loading.

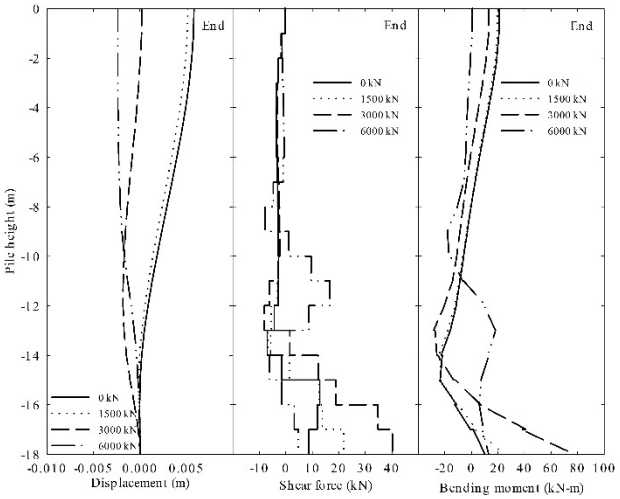

Fig. 7. Pile response profiles at the end of shaking.

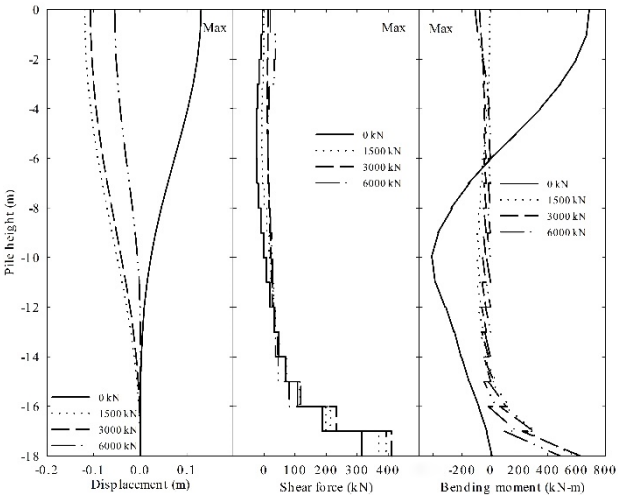

Fig. 8. Maximum pile response profiles during the shaking.

4. Comments on buckling load

For all the cases examined in the above numerical simulations, we notice the computed maximum bending moments in pile are not exceeding the yielding or plastic moments of the pile as shown in Table 2. This is indicative that the numerical simulations by OpenSeesPL do not predict the buckling of pile with the various assigned axial loadings (0~6000 kN).

As mentioned in the literature review, the buckling of piles in liquefiable ground can also be assessed by Bhattacharya's approach (2015), which considers the

unsupported pile length (D_L) due to soil liquefaction and the critical pile length (H_C) based on Euler's theory.

Results of the numerical simulations show the deposit soil will liquefy from the ground surface up to a depth of 12~18 m due to the assigned seismic shaking for the pile axial loads of 0~3000 kN. For the pile axial load of 6000 kN, the liquefied soil will reach to a depth of 6~12 m. In accordance, it can be estimated the unsupported pile lengths (D_L) would be approximately 18 m and 12 m, respectively, for the pile axial loadings of <3000 kN and 6000 kN.

By applying Eq. (4), the critical pile lengths (H_C) can be computed with the values of ∞, 20.2, 14.3 and 10.1 m, respectively, for the pile axial loads of 0, 1500, 3000 and 6000 kN.

Hence, Bhattacharya's approach would predict no buckling failure for piles with axial loads less than 3000 kN (i.e., $H_C > D_L$). For axial loads greater than 3000 kN, however, the piles will be buckling (i.e., $H_C < D_L$).

It is apparent that the predictions by numerical simulations using OpenSeesPL are not consistent with those of Bhattacharya's approach. As mentioned previously, OpenSeesPL consists of a 3D formulation of finite element method which considers interaction of pile and surrounding soil due to seismic shaking. Although the application of axial load on pile is permitted, if the axial load on pile deflection or buckling being properly considered in the software is still uncertain. On the other hand, Bhattacharya's approach neglects the confining effect of the liquefied soil and assumes a pseudo-static way for the dynamic inertial forces. It is not sure, however, if Bhattacharya's approach would be too conservative. Hence, further studies are warranted to justify the queries raised above.

Conclusions

This study was conducted to explore the influence of pile axial load on the responses of pile and surrounding soil due to seismic shaking. A 3-D finite element software, OpenSeesPL, was employed for the numerical simulations. Results of the study are listed below:

a. An increase in axial loading would generally decrease the lateral displacement and increase the bending moment of piles.
b. An increase in axial loading would reduce the acceleration and excess pore pressure responses in soils during seismic shaking and soil liquefaction.
c. Numerical simulations using OpenSeesPL indicate the piles with various assigned axial loads will be safe from buckling failure, with computed bending moments less than the yielding and plastic moments of the pile. However, these predictions are dissimilar with those by Bhattacharya's approach, indicating more studies are warranted for the analysis of pile buckling issue in liquefiable ground due to seismic shaking.

References

1) Adalier, K. and Elgamal, A. (2004) Mitigation of liquefaction and associated ground deformations by stone columns. Journal Engineering Geology, 72 (3-4), 275-291
2) Asgari, A., Oliaei, M., Bagheri, M. (2013) Numerical simulation of improvement of liquefiable soil layer using stone column and pile-pinning techniques. Soil Dynamics and Earthquake Engineering, 51, 77-96, doi: 10.1061/j.soildyn.2013.04.006
3) Bhattacharya, S. (2003) Pile instability during earthquake liquefaction. Ph.D. thesis. University of Cambridge, UK
4) Bhattacharya, S. (2015) Safety assessment of piled buildings in liquefiable soils: Mathematical tolls. Encyclopedia of Earthquake Engineering, doi: 10.1007/978-3-642-361975-5_232-1
5) Bhattacharya, S. and Goda, K. (2013) Probabilistic buckling analysis of axially loaded piles in liquefaction soil. Soil Dynamics and Earthquake Engineering, 45, 13-24
6) Bhattacharya, S. and Madabhushi, S.P.G. (2008) A critical review of methods for pile design in seismically liquefiable soils. Bulletin of Earthquake Engineering, 6 (3), 407-446
7) Bhattacharya, S. Madabhushi, S.P.G., Bolton, M.D. (2004) An alternative mechanism of pile failure in liquefiable deposits during earthquakes. Geotechnique, 54 (3), 203-213
8) Bhattacharya, S., Sarkar, R., Huang, Y. (2013) Seismic design of piles in liquefiable soils. New Frontiers in Engineering Geology and the Environment. Proceedings of the International Symposium on Coastal Engineering geology, ISCEG-Shanghai, 31-44
9) Boulanger, R.W. and Tokimatsu, K., Eds. (2005) Seismic performance and simulation of pile foundations in liquefied ana laterally spreading ground. Geotech. Spec. Publ., Special Publication GSP 145
10) Boulanger, R.W., Chang, D., Brandenberg, S.J., Armstrong, R.J., Kutter, B.L. (2007) Seismic design of pile foundations for liquefaction effects. Proc. 4th Int. Conf. on Earthquake Geotechnical Engineering-Invited Lectures, K.D. Pitilakis, ed., Springer, New York
11) Bowles, J.E. (1996) Foundations analysis and design. 5th Edition. McGraw-Hill, New York
12) Cubrinovski, M. and Ishihara, K. (2005) Assessment of pile group response to lateral spreading by single pile analysis. Proceedings of Workshop: Seismic Performance and Simulation of Pile Foundations in Liquefied and Laterally Spreading Ground (Geotechnical Special Publication (GSP) No. 145) (Editions R.W. Boulanger and K. Tokimatsu). American Society of Civil Engineers, Reston, VA, USA, 242-254
13) Dash, S.R., Bhattacharya, S., Blackeborough, A. (2010) Bending-buckling interaction as a failure mechanism of piles in liquefiable soils. Soil Dynamics Earthquake Engineering, 30, 32-39
14) Earthquake Engineering Research Institute (1999) The Chi-Chi Taiwan earthquake of September 21, 1999. EERI Special Earthquake Report, EERI, Oakland, California, USA
15) Elgamal, A., Lu, J., Forcellini, D. (2009) Mitigation of liquefaction-induced lateral deformation in sloping stratum: Three-dimensional numerical simulation. Journal of Geotechnical and Geoenvironmental Engineering, 135 (11), 1672-1682, doi: 10.061/(ASCE)GT.1943-5606.0000137
16) Elgamal, A., Yan, L., Yang, Z., Conte, J.P. (2008) Three-dimensional seismic response of Humboldt bay bridge-foundation-ground system. Journal of Structural Engineering, 134 (7), 1165-1176, doi: 10.1061/(ASCE)0733-9445(2008)134:7(1165)
17) Eslami, A. and Fellenius, B.H. (1997) Pile capacity by direct CPT and CPTu methods applied to 102 case histories. Canadian Geotechnical Journal, 34 (6), 886-904, doi: 101.1139/cgj-34-6-886
18) Fellenius, B.H. (1990) Guidelines for static pile design: a continuing education short course text. Deep Foundation Institute. Hawthorne, NJ.
19) Fellenius, B.H. (2006) The red book-basics of foundation design. Available from http://www.fellenius.net/
20) Finn, W. and Fujita, N. (2002) Piles in liquefiable soils: seismic analysis and design issues. Soil Dynamics and Earthquake Engineering, 22 (9), 731-742
21) GEER (2019) Geotechnical reconnaissance: The 28 September 2018 M7.5 Palu-Donggala, Indonesia Earthquake. Geotechnical Extreme

Events Reconnaissance

22) Goble, G.G. and Rausche, F. (1979) Pile driveability calculations by CAPWAP. Proceedings of the Conference on Numerical Methods in Offshore Pile, 22-23 May 1979. Institution of Civil Engineers, London, 29-36
23) JRA (1996) Design Specifications of Highway Bridges, Part V: Seismic Design, Japan Road Association, Tokyo, Japan
24) Kimura, Y. and Tokimatsu, K. (2005) Buckling stress of steel pile with vertical load in liquefied soil. Journal of Structural and Construction Engineering, 73-78
25) Knappett, J.A. and Madabhushi, S.P.G. (2005) Modelling of liquefaction-induced instability in pile groups. Seismic Performance and Simulation of Pile Foundations in Liquefied and Laterally Spreading Ground (Geotechnical Special Publication (GSP) No. 145) (Editions R.W. Boulanger and K. Tokimatsu). American Society of Civil Engineers, Reston, VA, USA, 225-267
26) Kokusho, T. (1999) Water film in liquefied sand and its effects on lateral spread. Journal of Geotechnical and Geoenvironmental Engineering, 125 (10), 817-826, doi: 10.1061/(ASCE)1090-0241(1999)125:10(817)
27) Kramer, S.L. (1996) Geotechnical earthquake engineering. Prentice-Hall Civil Engineering and Engineering Mechanics Series. Upper Saddle River, NJ: Prentice Hall
28) Kulhawy, F.H. (1984) Limiting tip and side resistance, fact or fallacy. Proceedings of a Symposium on Analysis and Design of Pile Foundations, San Francisco, California, 1-5 October 1984, Edited by J.R. Meyer. American Society of Civil Engineers (ASCE) Geotechnical Division, New York, 80-98
29) Lu, J. (2006) Parallel finite element modeling of earthquake site response and liquefaction. Ph.D. thesis, University of California, San Diego, La Jolla, CA
30) Lu, J., Kamatchi, P., Elgamal, A. (2019) Using stone columns to mitigate lateral deformation in uniform and stratified liquefiable soil strata. International Journal of Geomechanics, 19 (5), doi: 10.1061/(ASCE)GM.1943-5622.0001397
31) Mazzoni, S., McKenna, F., Fenves, G.L. (2006) Open System for Earthquake Engineering Simulation (OpenSees) user manual. Berkeley, CA: Pacific Earthquake Engineering Research Center, University of California, Berkeley
32) McKenna, F., Scott, M., Fenves, G.L. (2010) Nonlinear finite-element analysis software architecture using object composition. Journal of Computing in Civil Engineering, 24 (1), 95-107, doi: 10.1061/(ASCE)CP.1943-5487.0000002
33) Meyerhof, G.G. (1976) Bearing capacity and settlement of pile foundations. Journal of Geotechnical Engineering Division, ASCE, 102 (2), 195-228
34) Mitchell, J.K., Cooke, H.G., Shaeffer, J.A. (1998) Design considerations in ground improvement for seismic risk mitigations. Proc. Geotechnical Earthquake Engineering and Soil Dynamics III, Geotechnical Special Publication No. 75, Vol. 1, ASCE, Seattle, 1, 580-613
35) Poulos, H.G. (1989) Pile behavior-theory and application. Geotechnique. 39 (3), 365-415, doi:10.1680/geot.1989.39.3.365.
36) Rausche, F., Goble, G.G., Likins, G. (1985) Dynamic determination of pile capacity. Journal of Geotechnical Engineering, 111 (3), 367-383, doi: 10.1061/(ASCE)/0733-9410(1985)111:3(367)
37) Salgado, R. (2008) The engineering of foundations. McGraw-Hill, New York
38) Schmertmann, J.H. (1978) Guidelines for cone penetration test performance and design. US Department of Transportation. Federal Highway Administration. Offices of Research and development, Washington D.C. Report No. FHWA-TS-78-209
39) Shanker, K., Basudhar, P., Patra, N. (2007) Buckling of piles under liquefied soil conditions. Geotechnical and Geological Engineering, 25 (3), 303-313
40) Tang, L., Cong, S., Ling, X., Lu, J., Elgamal, A. (2015) Numerical study on ground improvement for liquefaction mitigation using stone columns encased with geosynthetics. J. Geotext. and Geomem., 43, 190-195, doi: 10.1016/j.geotexmem.2014.11.011
41) Terzaghi, K (1943) Theoretical soil mechanics. John Wiley and Sons Inc., New York
42) Wang, N. (2015) Three-dimensional modeling of ground-pile systems and bridge foundations. Ph.D. thesis, University of California, San Diego, La Jolla, CA
43) Yang, Z. and Elgamal, A. (2002) Influence of permeability on liquefaction-induced shear deformation. Journal of Engineering Mechanics, 128 (7), 720-729, doi: 10.1061/(ASCE)0733-9399(2002)128:7(720)
44) Yang, Z., Elgamal, A., Parra, E. (2003) A computational model for cyclic mobility and associated shear deformation. Journal of Geotechnical and Geoenvironmental Engineering, 129 (12), 1119-1127, doi: 10.1061/(ASCE)1090-0241(2003)129:12(1119)